Int. J. Morphol.,
43(6):1897-1908, 2025.

Fruits of *Hyphaene thebaica* L. for the Treatment of Hepatocellular Carcinoma: A Network Pharmacology and Molecular Docking Study

Frutos de *Hyphaene thebaica* L. para el Tratamiento de Carcinoma Hepatocelular: Un Estudio de Farmacología en Red y Acoplamiento Molecular

Nael Abutaha[1]; Mohamed A Wadaan[1] & Fahd A. AL-Mekhlafi[1]

ABUTAHA, N.; WADAAN, M. A. & AL-MEKHLAFI, F. A. Fruits of *Hyphaene thebaica* l. for the treatment of hepatocellular carcinoma: a network pharmacology and molecular docking study. *Int. J. Morphol., 43(6)*:1897-1908, 2025.

SUMMARY: Liver cancer is a major health challenge worldwide due to its high mortality rates. This study investigates the therapeutic potential of *Hyphaene thebaica* (Doum Palm) fruit extracts. Ultrasonic-assisted extraction using ethanol: HCl (1 % v/v) yielded the highest phenolic content (52.3 ± 2.1 mg GAE/g DW), while Soxhlet extraction with dichloromethane resulted in the highest lipid content (12.8 ± 0.5 %). The antioxidant potential of the acetone extract was notable, achieving an EC_{50} of 129 µg/mL. Cytotoxicity analysis against HuH-7 liver carcinoma cells revealed a significant dose-dependent effect, with dichloromethane extract demonstrating the highest cytotoxicity (IC_{50}: 155 µg/mL). Morphological studies confirmed apoptosis via DAPI and AO/EtBr staining. Bioinformatics analysis identified 423 common targets between 453 compound-related and 1,249 liver-related genes. Key hub genes, including *AKT1, TP53, EGFR, SRC,* and *IL6*, were identified through protein-protein interaction networks and GO/KEGG enrichment. Molecular docking studies showed a1-Sitosterol and 9, 19-Cyclolanost-24-en-3-ol had strong binding affinities with docking scores of -10.3 and -9.6 kcal/mol, respectively. These findings highlight the potential of *H. thebaica* fruit extracts as a source of bioactive compounds with antioxidant and anticancer properties, paving the way for further pharmaceutical research and development.

KEY WORDS: Antioxidant; Cytotoxicity; *Hyphaene thebaica*; Liver cancer; Molecular docking; Network pharmacology.

INTRODUCTION

Hepatocellular carcinoma (HCC) is a global health burden, representing the most prevalent form of primary liver cancer and ranking as one of the leading contributor to cancer-associated mortality (Baumeister *et al*., 2019). The disease accounts for approximately 90 % of liver cancer cases and is often associated with underlying liver conditions such as non-alcoholic fatty liver disease, chronic hepatitis B and C infections, and cirrhosis (Younossi & Henry, 2021; Gujarathi *et al*., 2025). Despite the availability of various therapeutic interventions, including surgery, chemotherapy, and targeted therapies, the prognosis for HCC patients remains dismal, with a five-year survival rate of less than 20 % in advanced stages (Villanueva & Llovet, 2011; Lee *et al*., 2012). Challenges such as late diagnosis, drug resistance, and adverse side effects of conventional treatments necessitate the exploration of novel, safe, and effective therapeutic alternatives (Petrowsky *et al*., 2020).

Natural products have long served as an invaluable provider of bioactive compounds for drug discovery, particularly in cancer research (Yang *et al*., 2025). Plants, in particular, have evolved to produce diverse metabolites that exhibit a wide range of bioactivities, including anticancer (Yang *et al*., 2025), anti-inflammatory (Gautam & Jachak, 2009), and antioxidant properties (Guo, 2025). Among these, *H. thebaica*, commonly known as Doum palm, is a fruit-bearing plant native to regions of Africa and the Middle East (Adenowo *et al*., 2024). Traditionally, *H. thebaica* has been used in folk medicine to manage various ailments, including postpartum hemorrhage and as a hematinic suspension. Doum tea is believed to help manage diabetes in Egypt. The resin is used for its diaphoretic and diuretic properties, treating tapeworms and alleviating animal bites. The roots treat bilharzias, and charcoal from the seed kernel is used for eye sores in livestock (Farag & Paré, 2013; Khalil *et al*., 2020).

[1] Department Zoology, College of Science, King Saud University, Riyadh, Saudi Arabia.
FUNDING. This project was funded by Ongoing Research Funding program (ORF-2025-757), King Saud University, Riyadh, Saudi Arabia.

Received: 2025-06-16 Accepted: 2025-09-14

Emerging research on natural products has emphasized the importance of a holistic approach to understanding their therapeutic potential. Unlike synthetic drugs that target a single molecule, plant-derived compounds often exhibit multi-target effects, simultaneously modulating several pathways (Shin *et al*., 2018; Yang *et al*., 2025). Network pharmacology (NWP) offers a powerful tool to decode the complex interactions between bioactive compounds and biological networks (Doghish *et al*., 2023). By integrating chemical, genomic, and proteomic data, NWP enables the identification of key targets and pathways that mediate the therapeutic effects of natural products (Schenone *et al*., 2013; Poornima *et al*., 2016). This approach is valuable in understanding the polypharmacological nature of *H. thebaica*. Complementing NWP and molecular docking (MD) is a computational technique that predicts and analyses the binding interactions between bioactive compounds and target proteins. MD provides critical insights into the potential mechanisms of action of the compounds, paving the way for their validation as therapeutic candidates.

In this study, we employ a comprehensive NWP and MD approach to explore the potential of *H. thebaica* fruits in treating HCC. Our objectives are to identify and characterise the key bioactive compounds present in *H. thebaica* fruits using phytochemical data, predict their molecular targets and associated biological pathways through NWP, and validate the interactions between selected bioactive compounds and key target proteins involved in HCC using MD studies. This integrative approach aims to elucidate the molecular mechanisms of the therapeutic potential of *H. thebaica* and its suitability as a natural multi-target agent against HCC.

MATERIAL AND METHOD

Obtaining and preparation of doum palm fruits. Fruits of *H. thebaica* L. (Doum Palm), a member of the Arecaceae family, were sourced from a local market in Mecca, Saudi Arabia. A botanist identified the species, and a voucher specimen (Voucher No. PRC-Mak 010) was deposited at the Bioproduct Research Chair, Zoology Department, King Saud University. Upon acquisition, the fruits were thoroughly rinsed with tap water. The seeds were discarded, and the fruit pulp was ground into a fine powder using a commercial blender (LC Multifunctional Grinder, China). The resulting powder was stored in an airtight container at 4°C until extraction.

Ultrasonic-assisted extraction of plant material. Ten grams of powdered plant material were subjected to ultrasonic-assisted extraction using various solvents (Sigma-Aldrich, USA). The extraction was carried out in a 250 mL glass beaker, maintaining a solvent-to-plant material ratio of 1:10 (w/v). A total of 100 mL of extraction solvent was used including n-hexane, ethyl acetate, ethanol, 70 % ethanol, ethanol: HCl (1 % v/v), and chloroform: methanol (2:1). The mixture was placed in an ultrasonic bath (WiseClean, Korea) and subjected to sonication at 40 kHz with a power output of 510 watts, and the temperature was monitored to ensure it remained at 40 °C. The sonication was carried out for 30 minutes. After extraction, the mixture was filtered using filter paper, and the filtrate was collected. The solvent was evaporated using a rotary evaporator (Heidolph, Germany) at 40 °C. The resulting concentrated extract was transferred and stored (4 °C) until further analysis.

Lipid extraction using soxhlet apparatus. Lipid extraction was performed using a Soxhlet apparatus with three solvents: n-hexane, dichloromethane, and acetone. A dried sample (30 g) was placed in a cellulose thimble, and 450 mL of each solvent was used for the extraction. The process was carried out for 6 hours under constant heating at 80 °C to facilitate continuous solvent reflux. Upon completion, the solvents were evaporated (Heidolph, Germany) and stored at 4°C for subsequent analysis.

Radical scavenging activity. The radical scavenging activity was evaluated following the method described by Abutaha *et al*. (2024). The effective concentration (EC50) was determined as the concentration required to achieve a 50 % reduction in DPPH· absorbance relative to the control. Extracts were prepared in DMSO at concentrations ranging from 0.05 to 1.25 mg/mL. For each sample, 10 µL of the extract was added to 190 µL of a freshly prepared 0.004 % DPPH· solution in methanol in a 96-well microplate. The control consisted of 10 µL of DMSO mixed with 190 µL of the DPPH· solution. The reaction mixtures were kept in the dark at 25 °C for 30 min. After the incubation, the absorbance was measured at 516 nm using a ChroMate microplate spectrophotometer (USA). The percentage of radical scavenging activity was calculated, and EC_{50} values (mg/mL) were derived through non-linear regression analysis utilizing OriginPro 8.5 software (USA). The results are presented as the mean ± standard deviation (SD) from three independent experimental replicates.

Determination of total phenolic content (TPC). The TPC was determined by adding 2 µL of each sample extract or gallic acid standard, prepared in methanol, to a 96-well microplate. Subsequently, 20 µL of Folin-Ciocalteu reagent was introduced into each well. After a 5-minute incubation period at 25 °C, 80 µL of 7.5 % sodium carbonate solution was added to initiate the reaction. The microplate was then incubated for an additional 30 min at 25 °C in the absence of light. Absorbance measurements were recorded at 765 nm. A standard curve of gallic acid (0–900 µg/mL) was prepared, and the TPC values were expressed as gallic acid equivalents (GAE) per gram of dry weight (mg GAE/g DW). All measurements were conducted in triplicate.

Cell lines and culture conditions

Cytotoxicity evaluation of *H. thebaica* extracts. HuH-7 cells (human liver carcinoma), procured from DSMZ, were cultured in DMEM supplemented with 10 % fetal bovine serum (FBS), 100 U/mL penicillin, and 100 µg/mL streptomycin. The cells were maintained at 37 °C in a humidified atmosphere containing 5 % CO_2 and 95 % air. Cells were harvested using trypsinisation for cytotoxicity assessment and seeded in 96-well plates at one cell per well. The plates were incubated under the same conditions for 24 hours before treatment. Various concentrations (0.000916 – 3.75 mg/mL) were prepared by diluting stock solutions in the culture medium. Each extract concentration was tested in triplicate. The cytotoxic effects of the extracts were assessed using the MTT assay. This method quantifies cell viability based on the reduction of the yellow dye 3-(4,5-dimethyl-2-thiazolyl)-2,5-diphenyl-2H-tetrazolium bromide (MTT) to a blue formazan product by metabolically active cells. After 72 hours of incubation, the medium in each well was replaced with 20 µL of MTT solution (5 mg/mL in PBS), and the plates were incubated for an additional 4 hours under the same conditions. The MTT solution was then removed, and the resulting formazan crystals were dissolved in 100 µL of isopropanol (0.01 % HCL) with gentle shaking. Absorbance was measured at 570 nm using an ELISA reader. The IC_{50} value, defined as the concentration of extract required to inhibit cell growth by 50 % compared to untreated controls, was determined for each extract.

Morphological analysis of cancer cells

Phase-contrast microscopy. Huh-7 cells were plated as reported earlier in a 24-well plate to examine cellular morphology and incubated in a CO_2 chamber. The following day, cells were exposed to the dichloromethane extract at 200 µg/mL). After 24 hours of treatment, cellular morphology was assessed using an inverted phase-contrast microscope (Leica, Germany).

DAPI Nuclear Staining. The HuH-7 cells nuclear morphology was assessed using DAPI staining to evaluate apoptosis and nuclear changes. Huh-7 cells were plated in 24 well plates as previously described by Abutaha *et al*. (2024) and treated with the dichloromethane extract (200 µg/mL) for 24 hours. The cells were washed with PBS and fixed with ice-cold ethanol after treatment. Fixed cells were stained with 1 µg/mL Hoechst solution. Excess dye was removed through PBS washes, and the stained cells were examined under a fluorescent microscope (EVOS, USA) to observe nuclear alterations.

Apoptosis detection using AO/EtBr staining. The dual staining method involving (AO) and (EtBr) was used to detect. HuH-7 cells were seeded (1×10^5 cells/well) in 24-well plates and incubated overnight. After attachment, cells were treated with 200 µg/mL of the dichloromethane extract for 24 hours. Post-treatment, cells were stained with 1 µL of freshly prepared AO/EtBr solution (AO: 5 µg/mL, EtBr: 5 µg/mL) (Abutaha *et al*., 2024). Stained cells were immediately analyzed under a fluorescence microscope (EVOS, USA).

Network pharmacology

Target collection and prediction. The potential targets of the phytocompounds were predicted using Swiss Target Prediction www.swisstargetprediction.ch/) to identify likely protein targets (Daina *et al*., 2019). Multiple databases were used to uncover genes potentially associated with hepatocellular carcinoma. These included DisGeNET, which provides information on disease-associated genes (www.disgenet.org/); GeneCards, an integrative database for human gene information (*www.genecards.org/*); PharmGKB, a resource for pharmacogenomics (*www.pharmgkb.org/*); and Liverome, which focuses on liver-specific genes (*liverome.kobic.re.kr/index.php*). To identify overlapping targets between the active compounds and hepatocellular carcinoma, Venn diagrams were generated using an online visualization tool (*www.bioinformatics.com.cn/*), highlighting shared targets for further analysis.

Protein-protein interaction (PPI) and component–target–pathway network. After identifying the intersecting targets, a protein-protein interaction (PPI) network was constructed using STRING (string-db.org/) (The Gene Ontology Consortium, 2017). The component–target–pathway relationships were further visualized through a network diagram created with Cytoscape software (version 3.10.3).

GO enrichment and KEGG analysis. ShinyGO 0.81 (https://bioinformatics.sdstate.edu/go/) was used to perform GO function and KEGG pathway enrichment analyses with Homo sapiens as the selected species. The FDR cutoff (False Discovery Rate cutoff) for all GO enrichment and pathway analyses was set as $p < 0.05$. The top-ranked pathways were integrated and plotted as the final pathway map.

Molecular docking. Ligands (phytocompounds) were downloaded from PubChem in structure data file (SDF) format and converted to PDB format using Open Babel 2.3.2. These ligands were further processed with AutoDock 4.2 to generate 'pdbqt' files for MD. The X-ray crystal structures of 10 target proteins AKT1 (1UNR), IL6 (1ALU), SRC (2SRC), TP53 (1TUP), EGFR (1M17), STAT3 (1BG1), PPARG (3CS8), BCL2 (2W3L), ESR1 (1A52), and PTGS2 (COX-2) (5F19) were retrieved from the Protein Data Bank (*www.rcsb.org*) and prepared for docking using

AutoDockTool-1.5.7. Preparation involved removing water molecules, adding polar hydrogens, and calculating Gasteiger charges. MD was conducted with AutoDock Vina 1.1.2, where grid coordinates were defined to facilitate site-specific docking. For each ligand-receptor interaction, nine binding conformations were generated and ranked based on binding energy. The most favorable conformations, determined by binding energy, were analyzed to identify key molecular interactions. These interactions were visualized using PyMOL and Discovery Studio Visualizer, providing insights into the ligand-receptor binding mechanisms.

RESULTS

Yield and Total Phenolic Content (TPC). The TPC and yield varied significantly among the extraction methods. For sonication extractions, the TPC followed this order: 70 % ethanol (15.5 ± 0.09 mg GAE/g) > ethanol: HCl (8.4 ± 0.01 mg GAE/g) > chloroform: methanol (2.3 ± 0.06 mg GAE/g) > ethanol (1.9 ± 0.13 mg GAE/g) > ethyl acetate (1.4 ± 0.02 mg GAE/g) > n-hexane (0.0 ± 0.0 mg GAE/g). The corresponding yields were: 70 % ethanol (2.62 g) > ethanol: HCl (1.8 g) > chloroform: methanol (0.334 g) > ethanol (0.244 g) > ethyl acetate (0.069 g) > n-hexane (0.020 g). For lipid extractions, the TPC was ranked as acetone (0.9 ± 0.02 mg GAE/g) > dichloromethane (0.12 ± 0.01 mg GAE/g) > n-hexane (0.05 ± 0.05 mg GAE/g), while the yield followed acetone (0.451 g) > dichloromethane (0.151 g) > n-hexane (0.098 g) (Table I).

Radical scavenging Activity. The radical scavenging activity, measured by EC50 values, showed varying antioxidant potential across extraction methods (Table I). In sonication-assisted extractions, n-hexane demonstrated a negligible antioxidant capacity. In contrast, ethyl acetate, ethanol, and 70 % ethanol exhibited antioxidant activity, with calculated EC50 of 0.355, 0.275, and 0.380 mg/mL, respectively. Ethanol: HCl and chloroform: methanol showed EC50 values of 0.292 mg/mL and 0.394 mg/mL, respectively. In lipid extractions, n-hexane had no EC_{50} value, dichloromethane showed an EC_{50} of 0.574 mg/mL, and acetone demonstrated the strongest antioxidant activity with an EC50 of 0.129 mg/mL.

Cytotoxicity assay. The IC_{50} toxicity assay results for Huh-7 cells varied across extraction methods and solvents. For the sonication method, n-hexane and ethyl Acetate extracts exhibited moderate cytotoxicity, with IC_{50} of 0.739 and 0.750 mg/mL, respectively. Ethanol, 70 % ethanol, and chloroform: methanol extracts showed negligible toxicity, with IC_{50} values exceeding 3.7 mg/mL. The ethanol: HCl extract displayed the highest toxicity among the sonication extracts, with an IC_{50} of 0.457 mg/mL. In contrast, lipid extraction yielded more cytotoxic compounds. Dichloromethane demonstrated the strongest toxicity, with an IC_{50} of 0.155 mg/mL, followed by n-hexane (0.236 mg/mL) and acetone (0.375 mg/mL). These findings suggest that lipid extraction methods are more effective at isolating potent bioactive compounds than the sonication method (Fig. 1).

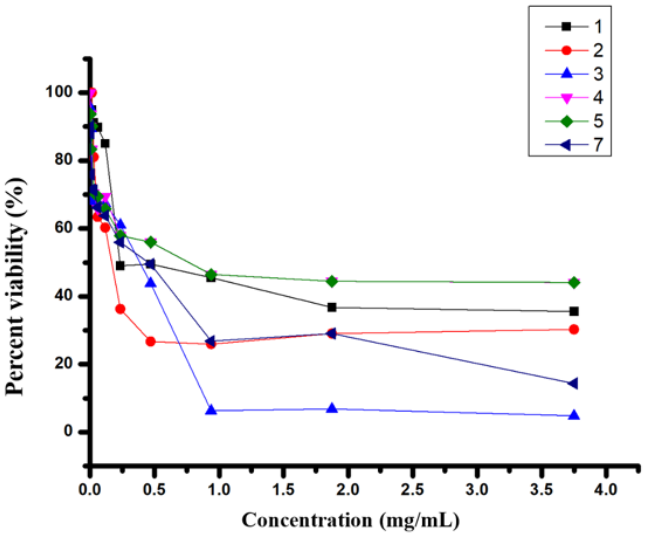

Fig. 1. The cytotoxic effects of various *H. thebaica* fruit extracts on HuH-7 cancer cell lines were evaluated after 48 hours of treatment. The extracts prepared via sonication included: (4) n-hexane, (5) ethyl acetate, and (7) ethanol:HCl. Those obtained using lipid extraction techniques comprised: (1) n-hexane, (2) dichloromethane, and (3) acetone.

Table I. Antioxidant Properties and Cytotoxic Effects of Extracts from *H. thebaica* Fruit. The table presents data on extraction methods, yields, total phenolic content, DPPH radical scavenging activity (EC_{50}), and cytotoxicity against HuH-7 cells (IC_{50}).

No.	Extraction Method	Yield in gram	TPC (mg GAE/g)	DPPH EC_{50} in mg\mL	IC_{50} mg/mL (Huh-7)
	Sonication method				
1	n-Hexane	0.020	0.0±0.0	0.0±0.0	0.739
2	Ethyl acetate	0.069	1.4±0.02	0.355±1.7	0.750
3	Ethanol	0.244	1.9±0.13	0.275±0.85	>3.7
4	70% ethanol	2.62	15.5±0.09	0.380±0.74	>3.7
5	Ethanol: HCL	1.8	8.4±0.01	0.292±0.74	0.457
6	Chloroform: Methanol	0.334	2.3±0.06	0.394±2.02	>3.7
	Lipid extraction				
7	n-Hexane	0.098	0.05±0.05	0.0±0.0	0.236
8	Dichloromethane	0.151	0.12±0.01	0.574±2.02	0.155
9	Acetone	0.451	0.9±0.02	0.129±0.85	0.375

DAPI staining. Nuclear fragmentation and chromatin condensation indicators were assessed in Huh-7 cells treated with dichloromethane extract using the DAPI staining assay. As shown in Figure 2, the extract induced distinct nuclear changes, including DNA condensation and chromatin alterations, in the treated cells. In contrast, control cells displayed no comparable effects.

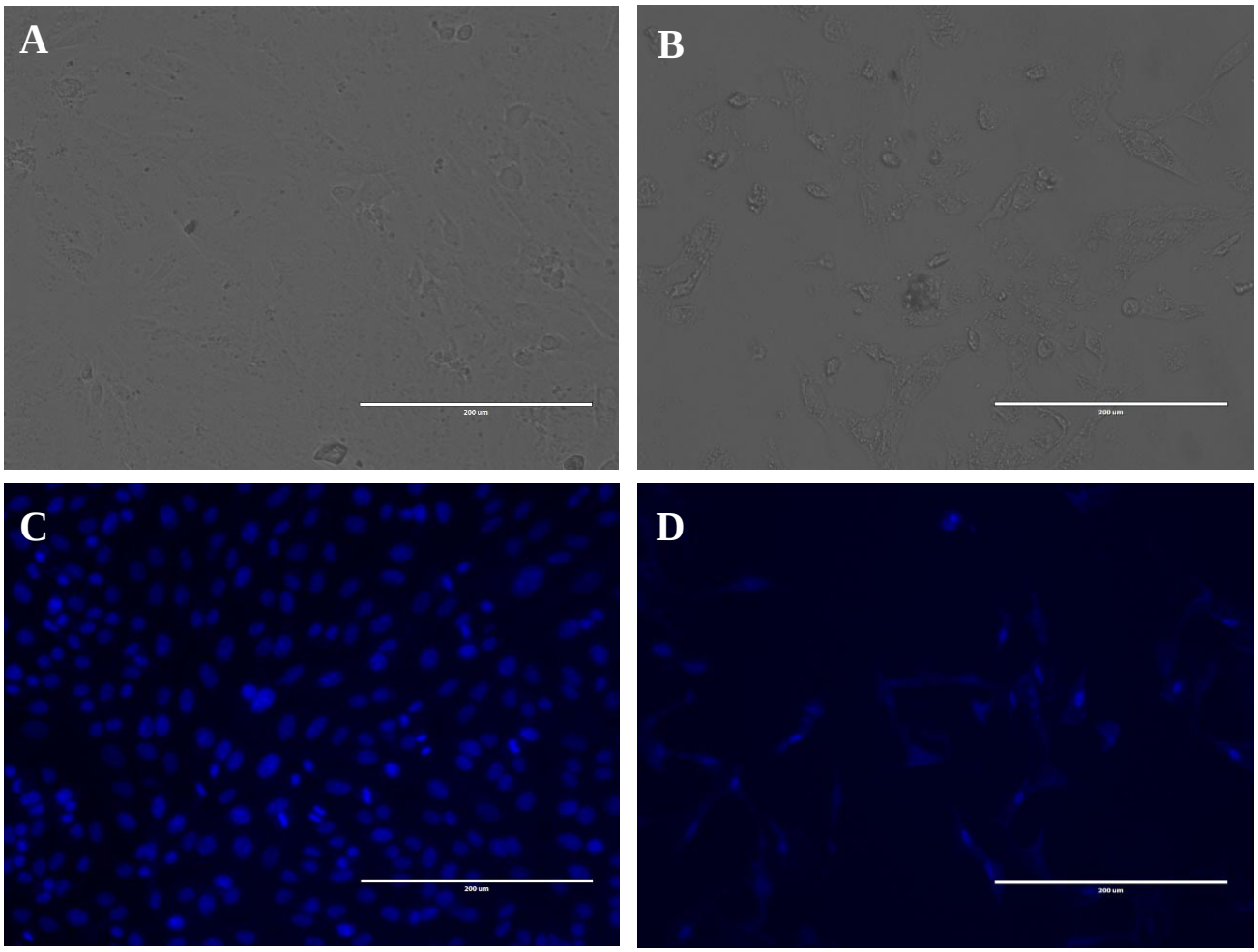

Fig. 2. Morphological assessment of *H. thebaica* dichloromethane extract effects on HuH-7 cells. (A) Untreated control and (B) cells treated with 200 µg/mL extract for 24 h, visualized by light microscopy. Fluorescence microscopy (excitation 435–485 nm) of Hoechst 33258-stained cells: (C) untreated control and (D) treated with 200 µg/mL *H. thebaica* extract. Scale bars: 200 µm.

AO- EtBr viability analysis. To assess early apoptosis, late apoptosis, and necrosis in HUH-7 cells following treatment with the dichloromethane extract, the cells were stained with (AO) and (EtBr) and observed under fluorescence microscopy. Untreated control cells, with intact membranes, were impermeable to EtBr and exhibited normal, round green-stained nuclei (Fig. 3). However, treatment with the extract induced significant apoptosis and/or necrosis. Apoptotic cells showed condensed or fragmented nuclei, with early-stage apoptosis characterized by green-stained nuclei impermeable to EtBr, and late-stage apoptosis marked by red-stained nuclei permeable to EtBr. Necrotic cells were identified by red-stained nuclei without evidence of nuclear condensation.

GC-MS analysis. The result revealed the presence of 17 compounds with varying area percentages. The most abundant compound was Lupeol (27.61 %), followed by n-Hexadecanoic acid (22.69 %) and a1-Sitosterol (11.52 %). Significant contributions were also observed from 9,12-Octadecadienoic acid (Z,Z)- (6.78 %) and 9,19-Cyclolanostan-3-ol, 24-methylene-, (3b)- (5.89 %). Among the fatty acids, n-Hexadecanoic acid dominated, with other notable fatty acids and derivatives including 9,12-Octadecadienoic acid (Z,Z)-, methyl ester (4.52 %), Dodecanoic acid (1.94 %), Tetradecanoic acid (0.83 %), and Hexadecanoic acid, methyl ester (0.87 %). Minor compounds such as (-)-Carvone (1.26 %) and 3-Dodecene (Z)- (1.07 %) were also detected (Table II).

Tabla II. GC-MS Analysis of Dichloromethane Extract of *Hyphaene thebaica* Fruit.

No	RT	Area %	Name	Molecular formula	Molecular weight
1	12.805	1.065787553	3-Dodecene, (Z)-	$C_{12}H_{24}$	168
2	14.261	1.256311421	(-)-Carvone	$C_{10}H_{14}O$	150
3	18.29	0.680063219	2-Dodecanol	$C_{12}H_{26}O$	186
4	21.611	1.476524655	Dodecanoic acid, methyl ester	$C_{13}H_{26}O_2$	214
5	22.921	1.940396429	Dodecanoic acid	$C_{12}H_{24}O_2$	200
6	27.229	0.827692479	Tetradecanoic acid	$C_{14}H_{28}O_2$	228
7	30.447	0.871087192	Hexadecanoic acid, methyl ester	$C_{17}H_{34}O_2$	270
8	31.201	22.69034778	n-Hexadecanoic acid	$C_{16}H_{32}O_2$	256
9	33.625	4.520034408	9,12-Octadecadienoic acid (Z, Z)-, methyl ester	$C_{19}H_{34}O_2$	294
10	33.76	2.355313248	9-Octadecenoic acid, methyl ester, (E)-	$C_{19}H_{36}O_2$	296
11	34.55	6.777223414	9,12-Octadecadienoic acid (Z, Z)-	$C_{18}H_{32}O_2$	280
12	34.848	2.273117697	cis-Vaccenic acid	$C_{18}H_{34}O_2$	282
13	34.975	1.980120662	Octadecanoic acid	$C_{18}H_{36}O_2$	284
14	41.027	6.268571566	9,19-Cyclolanost-24-en-3-ol, (3β)-	$C_{30}H_{50}O$	426
15	41.247	27.6098339	Lupeol	$C_{30}H_{50}O$	426
16	46.876	5.889702054	9,19-Cyclolanostan-3-ol, 24-methylene-, (3β)-	$C_{31}H_{52}O$	440
17	47.73	11.51787232	α1-Sitosterol	$C_{30}H_{50}O$	426

Target prediction screening of liver cancer-related targets. The gene targets associated with *H. thebaica* constituents were predicted through the SwissTargetPrediction databases, resulting in the prediction of 453 targets after post-elimination of duplicates for 17 phytochemicals. GeneCards, PharmGKB, Liverome, and DisGeNet databases were utilized to identify liver cancer-related targets. After eliminating duplicate entries, a total of 1,249 unique genes were identified. These genes were then compared with *H. thebaica*-related targets to determine overlapping and common gene targets associated with liver cancer. From this analysis, 423 target genes were selected based on the interaction between compound-associated gene targets and liver cancer-specific gene targets (Fig. 4).

Protein-Protein Interactions. STRING 12.0, an online tool, was utilized to identify PPIs. A total of 423 potential targets were considered, with Homo sapiens as the default organism. The network comprises 408 nodes and 5,697 edges, with a node degree of 27.9. The local clustering

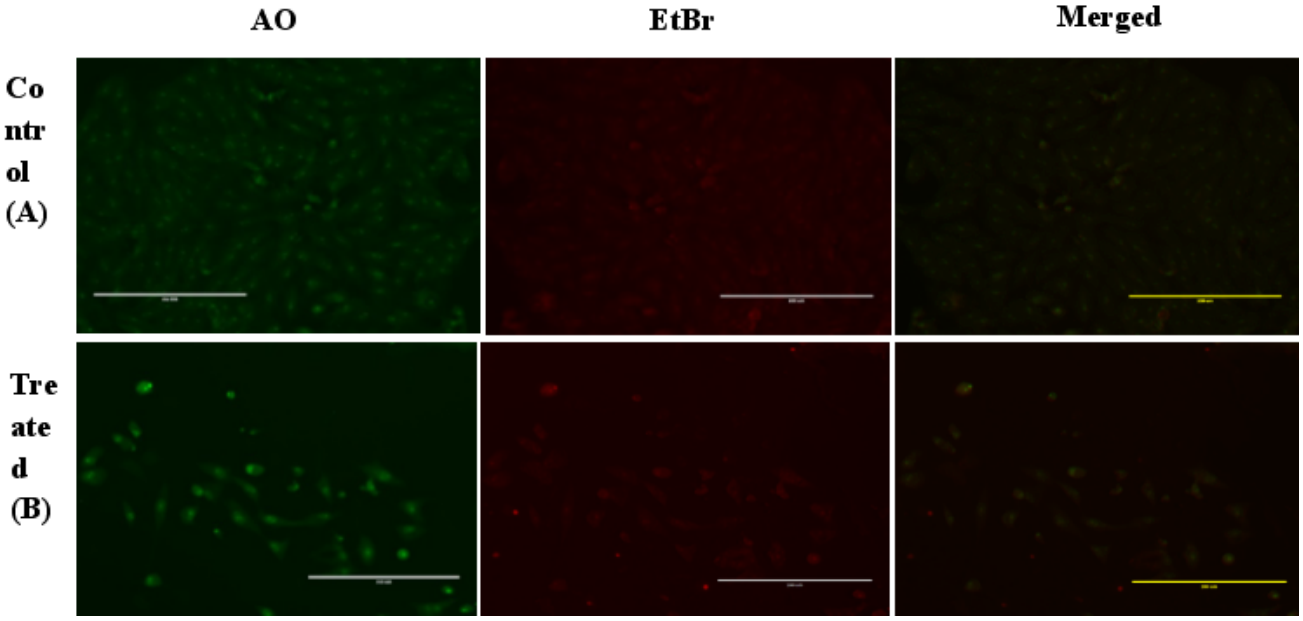

Fig. 3. AO/EtBr staining for apoptosis and necrosis detection in HUH-7 cells. (A) Negative control (untreated cells) showing viable cells with intact green-stained nuclei. (B) Cells treated with 200 µg/mL *H. thebaica* dichloromethane extract. Cells at 50 % confluency were treated for 24 h before staining and fluorescence microscopy analysis. Treated cells exhibited apoptotic morphology (condensed/ fragmented orange nuclei) and necrotic features (red-stained nuclei), while untreated controls maintained normal round nuclear morphology (green fluorescence), indicating membrane integrity and viability.

coefficient is 0.462, suggesting a tendency for nodes to form tightly-knit groups. Notably, the network contains significantly more edges than the expected 2,503, highlighting a high level of connectivity. This observation is further supported by a PPI (enrichment p-value of less than 1.0e-16 indicating a biologically meaningful association between the nodes. Subsequently, the Cytoscape software was utilized to compute the network parameters. The network analysis revealed 10 nodes and 45 edges, averaging 9.0 neighbors per node. The network exhibits a diameter and radius of 1, indicating that all nodes are directly connected. The characteristic path length is also 1.0, reflecting direct connectivity throughout the network. A clustering coefficient of 1.0 and a network density 1.0 demonstrate a fully connected, highly cohesive structure. The network heterogeneity and centralization are both 0.0, indicating uniformity in connectivity and the absence of dominant central nodes. The analysis identified a single connected component, confirming that the network is entirely connected (Fig. 4).

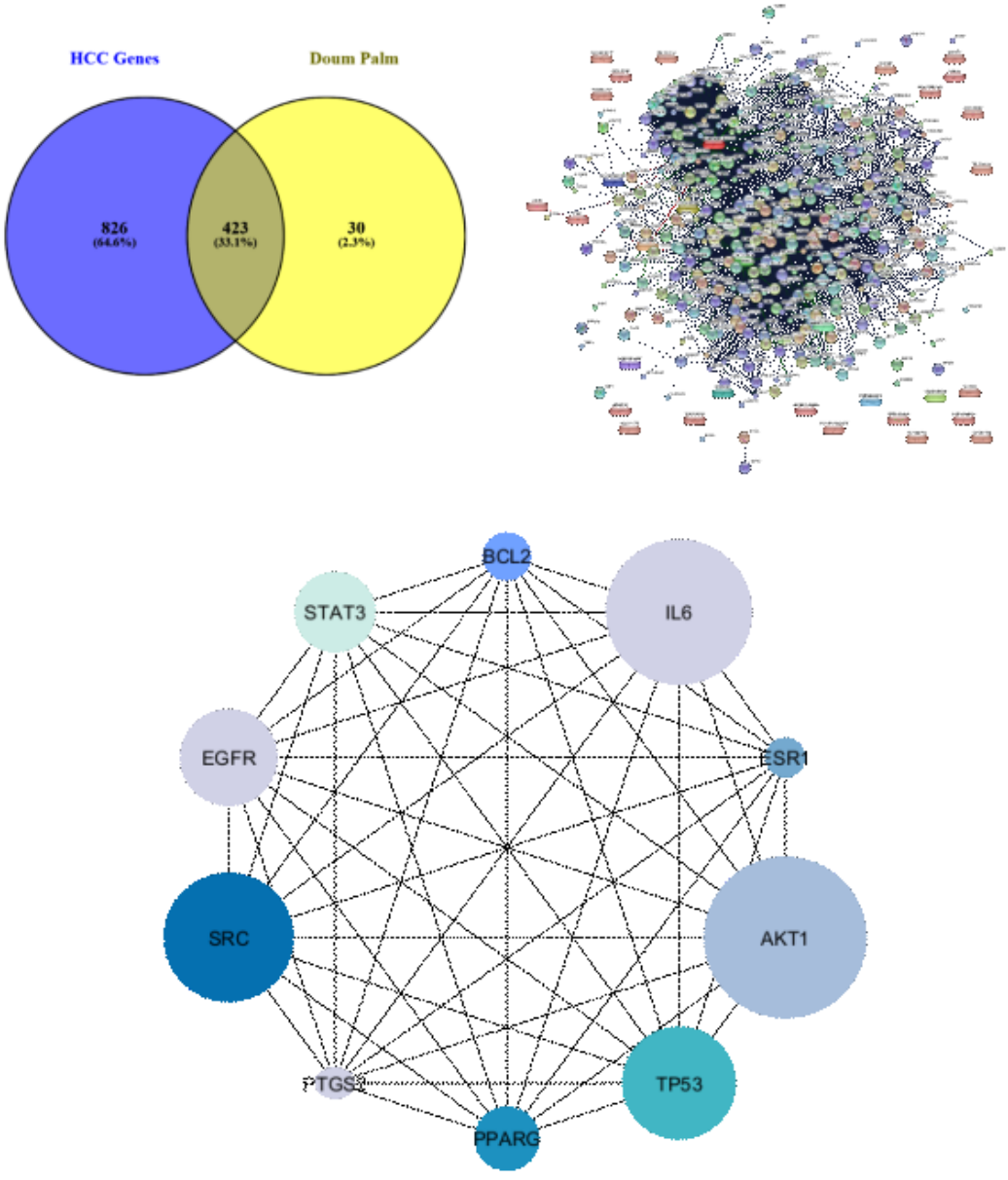

Fig. 4. Network pharmacology analysis of *H. thebaica* dichloromethane extract's potential therapeutic targets in liver cancer. (A) Venn diagram showing overlapping molecular targets between extract constituents and liver cancer proliferation markers. (B) Protein-protein interaction (PPI) network of identified potential therapeutic targets. (C) Focused view of the PPI network highlighting the top 10 hub targets (node size proportional to degree centrality), with key targets labeled for clarity.

Functional enrichment and pathway analysis. The analysis identifies ten key hub genes—AKT1, IL6, SRC, TP53, EGFR, STAT3, PPARG, BCL2, ESR1, and PTGS2 in liver cancer, highlighting their roles in tumor progression and therapeutic potential. These genes are enriched in biological processes such as miRNA-mediated gene silencing, chemical stress response, and post-transcriptional regulation, as well as pathways like PI3K/AKT, JAK-STAT, and HIF-1 signaling, all critical for cell survival, proliferation, and immune evasion. Cellular localization in transcription regulator complexes and plasma membrane rafts suggests their involvement in signaling hubs vital for cancer cell communication. Functionally, these genes regulate transcription factor binding, kinase activity, and ligand-activated receptor activity, driving tumor growth, angiogenesis, and metabolic dysregulation. For instance, AKT1 and EGFR activate downstream pathways promoting cell proliferation, while IL6 and STAT3 mediate immune suppression and inflammation. Tumor suppressor TP53, frequently mutated in liver cancer, disrupts apoptosis, complemented by anti-apoptotic BCL2 and inflammatory PTGS2 (Fig. 5).

Molecular docking. The molecular docking analysis evaluated the binding affinities of 18 compounds across 10 target proteins, revealing significant interaction variability (Fig. 5). The strongest binding was observed for a1-Sitosterol against 1M17, with a docking score of -10.3, highlighting its potential as a lead molecule. The 9,19-Cyclolanost-24-en-3-ol, (3β)- and Lupeol also exhibited notable binding affinities, with 9,19-Cyclolanost-24-en-3-ol, (3β)- showing strong interactions with 1M17 (-9.6), 2SRC (-8.8), and 1A52 (-8.4), while compound Lupeol demonstrated significant binding to 2SRC (-8.6), 1M17 (-8.9), and 1BG1 (-8.7). Compound 9,19-Cyclolanostan-3-ol, 24-methylene-, (3β)-also showed strong interactions with 2SRC (-8.7) and 1M17 (-8.5). In contrast, compound 18 (glycerol), used as a negative control, displayed weaker affinities with docking scores ranging between -3.1 and -4.3 across all targets. Notably, 1M17 emerged as the most promising protein target, with multiple compounds achieving docking scores below -8.5, including the strongest interaction. This study highlights the potential of a1-Sitosterol for further therapeutic development and suggests compounds 9,19-Cyclolanost-24-en-3-ol, (3β)- and Lupeol as versatile candidates for multi-target drug design.

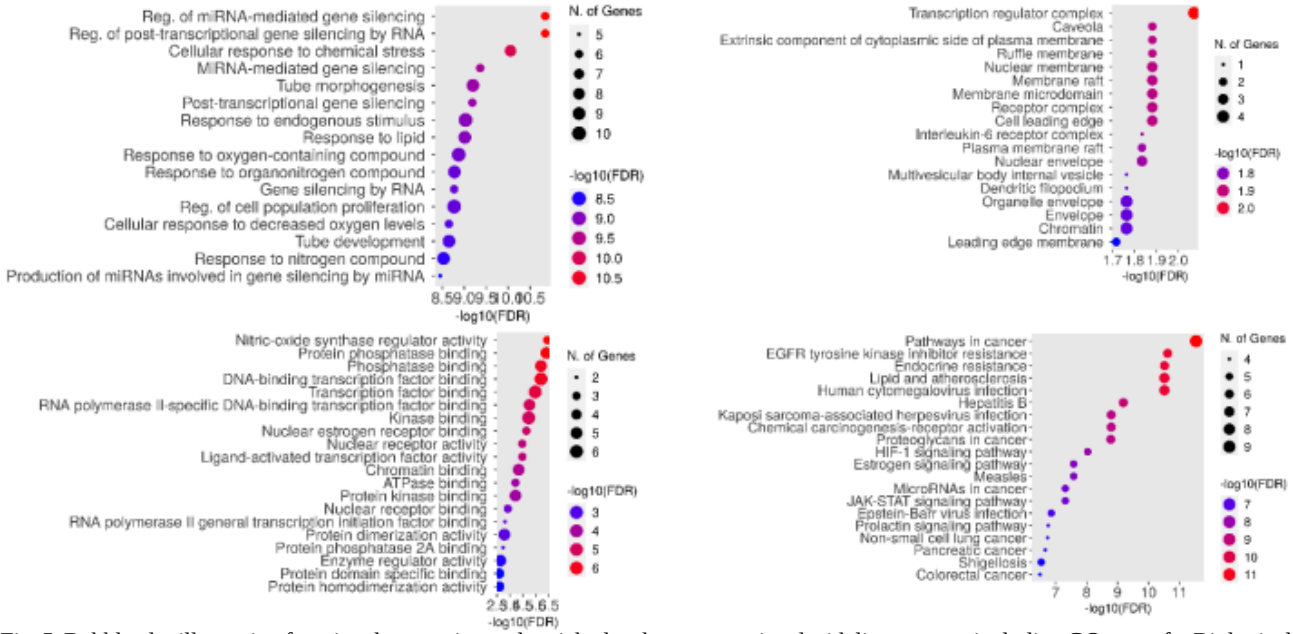

Fig. 5. Bubble plot illustrating functional annotation and enriched pathways associated with liver cancer, including GO terms for Biological Processes (BP), Cellular Components (CC), Molecular Functions (MF), and KEGG pathway analysis.

DISCUSSION

Numerous natural products have shown promise as cancer therapeutics, attributed to their diverse bioactive properties and therapeutic potential (Newman & Cragg, 2016). Terpenoids, phenols, alkaloids, flavonoids, glycosides, and peptides have been recognized for their notable anticancer properties, including suppressing the proliferation of malignant cells and inhibiting their metastatic progression (de Mejia & Dia, 2010). Natural compounds such as artemisinin, parthenolide, and thapsigargin are currently being investigated in clinical trials to assess their

effectiveness as potential cancer treatments (Laszczyk, 2009; Alotaibi *et al*., 2023). The present study used NWP-based analysis to identify cancer-related targets and pathways of *H. thebaica* dichloromethane extract and its phytochemical constituents. In addition, we confirmed the anticancer potential of *H. thebaica* extracts against HuH-7 cell lines by assessing cytotoxicity *in vitro*.

The results of our study revealed that the acetone extract exhibited the highest antioxidant activity, with an IC50 value of 129 µg/mL. This value is lower than those obtained using other solvents in sonication and Soxhlet extraction methods, highlighting the efficiency of acetone in extracting antioxidant compounds. However, another study reported the lowest IC50 values of 52.21 µg/mL for ethyl acetate extract (Dahiru & Nadro, 2022) and 76.8 µg/mL for 80 % methanol extract (Taha *et al*., 2020), indicating these extracts demonstrated the highest antioxidant activity overall. Notably, that study did not involve heat treatment or sonication, underscoring the significant influence of extraction methods on the antioxidant activity of plant extracts. While heat treatment and sonication are commonly used to enhance the extraction of bioactive compounds, some studies have shown that under certain conditions, these techniques can adversely affect phenolic content and antioxidant activity (Xu *et al*., 2007; Annegowda *et al*., 2010).

In-depth evaluation of the dichloromethane extract derived from *H. thebaica* revealed its ability to trigger apoptosis in liver cancer cells. Apoptotic cell death is characterized by specific morphological alterations, including cell rounding, shrinkage, chromatin condensation within the nucleus, and detachment from the substratum (Doonan & Cotter, 2008). The present study observed significant morphological changes in liver cancer cells following treatment with the extract. In contrast, the control group maintained their normal morphology, adhered to the culture surface, and displayed a confluence rate of 95-100 %.

The nuclei of control cells stained with DAPI appeared uniform in size and shape. However, nuclei in the dichloromethane-treated cells shoed significant abnormalities, including condensation, shrinkage, and fragmentation. These alterations suggest that the dichloromethane extract induces apoptosis in liver cancer cells. To further validate these results, AO-EtBr dual staining was conducted. In control, HuH-7 cells (Fig. 6), green fluorescence signified intact nuclei and preserved membrane

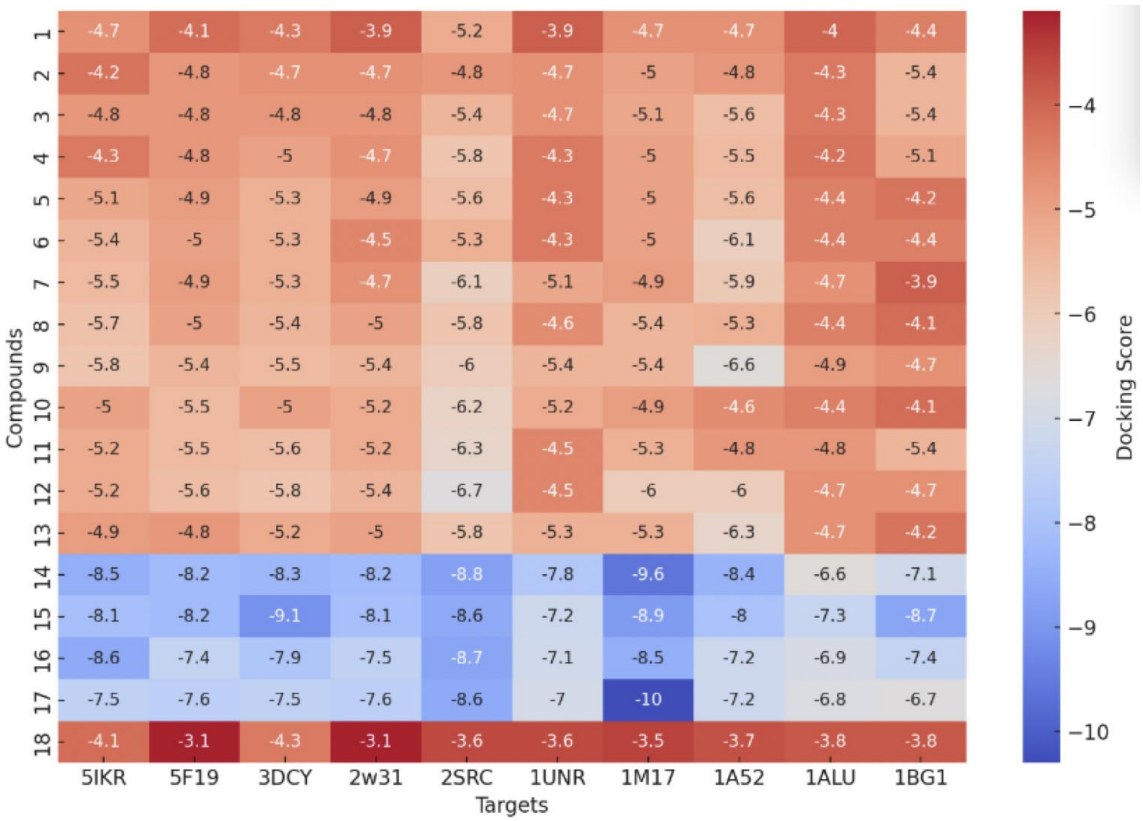

Fig. 6. Heatmap illustrating the binding affinities of bioactive compounds from Dichloromethane Extract of *H. thebaica* against a range of protein targets, calculated using AutoDock Vina. Binding energies are expressed in kcal/mol, with numerical values indicating the strength of interactions.

integrity without red fluorescence. In contrast, cells treated with the dichloromethane extract displayed reduced viability and increased apoptotic markers, such as bright green and yellow-orange fluorescence, signaling chromatin condensation and compromised cell membranes. Since apoptosis is a crucial mechanism for cancer treatment, these findings highlight the potential of the dichloromethane extract as an effective inducer of apoptosis in liver cancer cells (Surh, 2003). Identifying agents such as the dichloromethane extract, which can efficiently induce apoptosis, is crucial for developing innovative anticancer therapies.

The identification of the ten hub genes AKT1, IL6, SRC, TP53, EGFR, STAT3, PPARG, BCL2, ESR1, and PTGS2 enhances our understanding of the molecular mechanisms driving hepatocellular carcinoma (HCC). These genes contribute to key dysregulated pathways and cellular processes, such as inflammation, apoptosis evasion, and genomic instability, accelerating HCC progression. Targeting these hub genes offers promising strategies for therapeutic intervention. AKT1, a central regulator of the PI3K/AKT/mTOR pathway, plays a crucial role in promoting cell growth, survival, and angiogenesis in liver cancer (Wang *et al*., 2013; Sun *et al*., 2021). Preclinical studies have shown that inhibitors like alpelisib can effectively curb tumor growth, underscoring the therapeutic potential of this pathway (Xu *et al*., 2021). TP53 mutations, found in over 50 % of HCC cases, highlight the challenge of genomic instability and apoptosis resistance (Pollutri *et al*., 2016). Restoring its wild-type function through gene therapies or small molecules remains a promising approach for treatment. The IL6/STAT3 axis exemplifies the role of inflammation in HCC, driving immune evasion and tumor growth (Middleton *et al*., 2014; Shin *et al*., 2018). Inhibitors like ruxolitinib, targeting STAT3, have shown promise in preclinical models, reducing inflammation and tumor progression (Johnson *et al*., 2018). Pathway enrichment analysis reveals the importance of PI3K/AKT, JAK/STAT, and HIF-1 signaling in tumor proliferation, hypoxia adaptation, and immune suppression (Wang *et al*., 2018; Bandopadhyay & Patranabis, 2023). Emerging therapeutic agents targeting these pathways, such as EZN-2968 for HIF-1, represent expanding options for HCC treatment (Greenberger *et al*., 2008). Additionally, miRNA-mediated gene silencing plays a significant role in HCC progression, as miRNAs like miR-122 and miR-21 modulate gene expression and contribute to hepatocarcinogenesis (Oura *et al*., 2020; Doghish *et al*., 2023). Anti-apoptotic proteins, such as BCL2, exacerbate resistance to therapies, making them crucial targets for drug development (Anchimowicz *et al*., 2025). PTGS2 (COX-2) overexpression in HCC promotes inflammation and tumor progression, and inhibitors like venetoclax and celecoxib have shown synergistic effects in preclinical models (Wang *et al*., 2024). Identifying EGFR as a key target in this study further strengthens the rationale for using tyrosine kinase inhibitors in HCC treatment (da Fonseca *et al*., 2020). Combining immune checkpoint inhibitors with strategies targeting the IL6/STAT3 pathway may help overcome immune suppression, offering a promising immunotherapeutic approach (Varayathu *et al*., 2021; Papavassiliou *et al*., 2023).

Incorporating MD results provides further validation of these therapeutic strategies. Among the evaluated compounds, α1-Sitosterol exhibited the strongest binding affinity to EGFR (PDB ID: 1M17), with a docking score of -10.3, indicating its potential as a lead compound for targeted therapy. Additionally, compounds like 9,19-Cyclolanost-24-en-3-ol (3β)- and Lupeol showed strong interactions with SRC (PDB ID: 2SRC) and ESR1 (PDB ID: 1A52), suggesting their potential for multi-target drug design. The docking results for 9,19-Cyclolanostan-3-ol, 24-methylene, (3β) further reinforce its relevance, particularly in interactions with SRC and EGFR, which emerged as promising therapeutic targets. The analysis identified EGFR (1M17) as the most significant protein target, given the consistent strong docking scores observed with multiple compounds. The inclusion of glycerol as a negative control, showing weaker affinities (-3.1 to -4.3), validates the specificity of the observed interactions.

While these MD results provide valuable insights into potential therapeutic agents, future studies should aim to experimentally validate these findings through *in vitro* and *in vivo* testing. Combinatorial strategies that integrate novel compounds with established therapies, such as venetoclax, celecoxib, and immune checkpoint inhibitors, should also be explored to enhance therapeutic outcomes in HCC. By combining biomarker discovery with MD, this study highlights the potential in liver cancer treatment, paving the way for more effective and targeted therapies.

By targeting these critical apoptotic pathways, the dichloromethane extract from *H. thebaica* could act synergistically with the hub genes identified in the previous discussion, offering a multi-targeted approach to treating liver cancer. The extract's ability to trigger apoptotic markers such as chromatin condensation and membrane rupture could reflect a broader impact on key signaling pathways, including those regulated by TP53, AKT1, BCL2, and PTGS2. As these pathways are often dysregulated in liver cancer, the dichloromethane extract may serve as a potent agent for restoring apoptosis and overcoming resistance mechanisms in HCC cells.

CONCLUSION

The study highlights the significant potential of the dichloromethane extract from *H. thebaica*, in cancer therapy. The extract demonstrated antioxidant activity and induced apoptosis in liver cancer cells, suggesting its promise as a therapeutic agent. The identification of key genes and pathways involved in HCC provides valuable insights for targeted therapy. Future research should focus on validating these findings through *in vitro* and *in vivo* studies and exploring combinatorial strategies to enhance therapeutic outcomes.

ACKNOWLEDGMENTS. The authors express their sincere appreciation to Ongoing Research Funding program (ORF-2025-757), King Saud University, Riyadh, Saudi Arabia.

ABUTAHA, N.; WADAAN, M. A. & AL-MEKHLAFI, F. A. Frutos de *Hyphaene thebaica* L. para el tratamiento del carcinoma hepatocelular: Un estudio de farmacología en red y acoplamiento molecular. *Int. J. Morphol., 43(6)*:1897-1908, 2025.

RESUMEN: El cáncer de hígado representa un importante problema de salud a nivel mundial debido a sus altas tasas de mortalidad. Este estudio investiga el potencial terapéutico de los extractos de fruto de *Hyphaene thebaica* (palma Doum). La extracción asistida por ultrasonidos con etanol: HCl (1 % v/v) arrojó el mayor contenido fenólico (52,3 ± 2,1 mg GAE/g PS), mientras que la extracción Soxhlet con diclorometano resultó en el mayor contenido lipídico (12,8 ± 0,5 %). El potencial antioxidante del extracto fue notable, alcanzando una CE_{50} de 129 µg/mL. El análisis de citotoxicidad contra células de carcinoma hepático HuH-7 reveló un efecto dosis-dependiente significativo, donde el extracto de diclorometano demostró la citotoxicidad más alta (CI_{50}: 155 µg/mL). Los estudios morfológicos confirmaron la apoptosis mediante tinción con DAPI y AO/EtBr. El análisis bioinformático identificó 423 dianas comunes entre 453 genes relacionados con compuestos y 1249 genes relacionados con el hígado. Los genes centrales clave, incluyendo AKT1, TP53, EGFR, SRC e IL6, se identificaron mediante redes de interacción proteína-proteína y enriquecimiento con GO/KEGG. Los estudios de acoplamiento molecular mostraron que el α1-sitosterol y el 9,19-ciclolanost-24-en-3-ol tenían fuertes afinidades de unión con puntuaciones de acoplamiento de -10,3 y -9,6 kcal/mol, respectivamente. Estos hallazgos resaltan el potencial de los extractos de fruto de *H. thebaica* como fuente de compuestos bioactivos con propiedades antioxidantes y anticancerígenas, lo que abre el camino para una mayor investigación y desarrollo farmacéutico.

PALABRAS CLAVE: Antioxidante; Citotoxicidad; *Hyphaene thebaica*; Cáncer de hígado; Acoplamiento molecular; Farmacología en red.

REFERENCES

Abutaha, N.; Alghamdi, R. & Al-Waddan, M. Induction of apoptosis and ROS production in liver cancer cells by saponin fraction from *Alcea rosea* L. seeds. *Indian J. Anim. Res., 58(10)*:1765-71, 2024.

Adenowo, A. F.; Ajagun-Ogunleye, O. M.; Salisu, T. F.; Olaleye-Haroun, O. S.; Omotayo, H. A. & Akinsanya, M. A. Broad-spectrum nutritional and pharmacological significance of the wild *Hyphaene thebaica* palm fruit. *J. Food Biochem., 2024*:8380215, 2024.

Alotaibi, N. M.; Alotaibi, M. O.; Alshammari, N.; Adnan, M. & Patel, M. Network pharmacology combined with molecular docking, molecular dynamics and *in vitro* validation reveals the therapeutic potential of *Thymus vulgaris* L. essential oil against human breast cancer. *ACS Omega, 8(50)*:48344-59, 2023.

Anchimowicz, J.; Zielonka, P. & Jakiela, S. Plant secondary metabolites as modulators of mitochondrial health: antioxidant, anti-apoptotic and mitophagic mechanisms. *Int. J. Mol. Sci., 26(1)*:380, 2025.

Annegowda, H. V.; Anwar, L. N.; Mordi, M. N.; Ramanathan, S. & Mansor, S. M. Influence of sonication on phenolic content and antioxidant activity of *Terminalia catappa* L. leaves. *Pharmacognosy Res., 2(6)*:368-373, 2010.

Bandopadhyay, S. & Patranabis, S. Mechanisms of HIF-driven immunosuppression in tumour microenvironment. *J. Egypt. Natl. Canc. Inst., 35(1)*:27, 2023.

Baumeister, S. E.; Schlesinger, S.; Aleksandrova, K.; Jochem, C.; Jenab, M.; Gunter, M. J.; Overvad, K.; Tjønneland, A.; Boutron-Ruault, M. C.; Carbonnel, F.; *et al*. Association between physical activity and risk of hepatobiliary cancers: a multinational cohort study. *J. Hepatol., 70(5)*:885-92, 2019.

da Fonseca, L. G.; Reig, M. & Bruix, J. Tyrosine kinase inhibitors and hepatocellular carcinoma. *Clin. Liver Dis., 24(4)*:719-37, 2020.

Dahiru, M. M. & Nadro, M. S. Phytochemical composition and antioxidant potential of *Hyphaene thebaica* fruit. *Borneo J. Pharm., 5(4)*:325-33, 2022.

Daina, A.; Michielin, O. & Zoete, V. SwissTarget Prediction: updated data and new features for efficient prediction of protein targets of small molecules. *Nucleic Acids Res., 47(W1)*:W357-W364, 2019.

de Mejia, E. G. & Dia, V. P. Role of nutraceutical proteins and peptides in apoptosis, angiogenesis and metastasis of cancer cells. *Cancer Metastasis Rev., 29(3)*:511-8, 2010.

Doghish, A. S.; Elballal, M. S.; Elazazy, O.; Elesawy, A. E.; Elrebehy, M. A.; Shahin, R. K. & Sallam, A.-A. M. Role of miRNAs in liver diseases: potential therapeutic and clinical applications. *Pathol. Res. Pract., 243*:154375, 2023.

Doonan, F. & Cotter, T. G. Morphological assessment of apoptosis. *Methods, 44(3)*:200-4, 2008.

Farag, M. A. & Paré, P. W. Phytochemical analysis and anti-inflammatory potential of *Hyphaene thebaica* L. fruit. *J. Food Sci., 78(10)*:C1503-C1508, 2013.

Gautam, R. & Jachak, S. M. Recent developments in anti-inflammatory natural products. *Med. Res. Rev., 29(5)*:767-820, 2009.

Greenberger, L. M.; Horak, I. D.; Filpula, D.; Sapra, P.; Westergaard, M.; Frydenlund, H. F.; Albaek, C.; Schrøder, H. & Ørum, H. RNA antagonist of hypoxia-inducible factor-1a (EZN-2968) inhibits tumor cell growth. *Mol. Cancer Ther., 7(11)*:3598-608, 2008.

Gujarathi, R.; Klein, J. A.; Liao, C. Y. & Pillai, A. Changing demographics and epidemiology of hepatocellular carcinoma. *Clin. Liver Dis., 29(1)*:1-15, 2025.

Guo, M. *Chapter 2 - Antioxidants and antioxidant-rich foods.* In: Guo, M. (Ed.). Functional Foods. Principles and Technology. Amsterdam, Elsevier, 2025. pp.7-53.

Johnson, D. E.; O'Keefe, R. A. & Grandis, J. R. Targeting the IL-6/JAK/STAT3 signalling axis in cancer. *Nat. Rev. Clin. Oncol., 15(4)*:234-8, 2018.

Khalil, O.; Ibrahim, R. & Youssef, M. Comparative assessment of phenotypic and molecular diversity in doum (*Hyphaene thebaica* L.). *Mol. Biol. Rep., 47(1)*:275-84, 2020.

Laszczyk, M. N. Pentacyclic triterpenes of the lupane, oleanane and ursane group as tools in cancer therapy. *Planta Med., 75(15)*:1549-60, 2009.

Lee, S. S.; Shin, H. S.; Kim, H. J.; Lee, S. J.; Lee, H. S.; Hyun, K. H.; Kim, Y. H.; Kwon, B. W.; Han, J. H.; Choi, H.; *et al*. Analysis of prognostic factors and 5-year survival rate in patients with hepatocellular carcinoma: a single-center experience. *Korean J. Hepatol., 18(1)*:48-56, 2012.

Middleton, K.; Jones, J.; Lwin, Z. & Coward, J. I. Interleukin-6: an angiogenic target in solid tumours. *Crit. Rev. Oncol. Hematol., 89(1)*:129-39, 2014.

Newman, D. J. & Cragg, G. M. Natural products as sources of new drugs from 1981 to 2014. *J. Nat. Prod., 79(3)*:629-61, 2016.

Oura, K.; Morishita, A. & Masaki, T. Molecular and functional roles of microRNAs in the progression of hepatocellular carcinoma: a review. *Int. J. Mol. Sci., 21(21)*:8362, 2020.

Papavassiliou, K. A.; Marinos, G. & Papavassiliou, A. G. Combining STAT3-targeting agents with immune checkpoint inhibitors in NSCLC. *Cancers (Basel), 15(2)*:386, 2023.

Petrowsky, H.; Fritsch, R.; Guckenberger, M.; De Oliveira, M. L.; Dutkowski, P. & Clavien, P. A. Modern therapeutic approaches for the treatment of malignant liver tumours. *Nat. Rev. Gastroenterol. Hepatol., 17(12)*:755-72, 2020.

Pollutri, D.; Gramantieri, L.; Bolondi, L. & Fornari, F. TP53/microRNA interplay in hepatocellular carcinoma. *Int. J. Mol. Sci., 17(12)*:2029, 2016.

Poornima, P.; Kumar, J. D.; Zhao, Q.; Blunder, M. & Efferth, T. Network pharmacology of cancer: From understanding of complex interactomes to the design of multi-target specific therapeutics from nature. *Pharmacol. Res., 111*:290-302, 2016.

Schenone, M.; Dancˇík, V.; Wagner, B. K. & Clemons, P. A. Target identification and mechanism of action in chemical biology and drug discovery. *Nat. Chem. Biol., 9(4)*:232-40, 2013.

Shin, J.; Prabhakaran, V. S. & Kim, K. S. The multi-faceted potential of plant-derived metabolites as antimicrobial agents against multidrug-resistant pathogens. *Microb. Pathog., 116*:209-214, 2018.

Sun, E. J.; Wankell, M.; Palamuthusingam, P.; McFarlane, C. & Hebbard, L. Targeting the PI3K/Akt/mTOR pathway in hepatocellular carcinoma. *Biomedicines, 9(11)*:1639, 2021.

Surh, Y. J. Cancer chemoprevention with dietary phytochemicals. *Nat. Rev. Cancer, 3(10)*:768-80, 2003.

Taha, G. A.; Abdel-Farid, I. B.; Elgebaly, H. A.; Mahalel, U. A.; Sheded, M. G.; Bin-Jumah, M. & Mahmoud, A. M. Metabolomic profiling and antioxidant, anticancer and antimicrobial activities of *Hyphaene thebaica*. *Processes, 8(3)*:266, 2020.

The Gene Ontology Consortium. Expansion of the Gene Ontology knowledgebase and resources. *Nucleic Acids Res., 45(D1)*:D331-D338, 2017.

Varayathu, H.; Sarathy, V.; Thomas, B. E.; Mufti, S. S. & Naik, R. Combination strategies to augment immune checkpoint inhibitors efficacy: implications for translational research. *Front. Oncol., 11*:559161, 2021.

Villanueva, A. & Llovet, J. M. Targeted therapies for hepatocellular carcinoma. *Gastroenterology, 140(5)*:1410-26, 2011.

Wang, C.; Cigliano, A.; Delogu, S.; Armbruster, J.; Dombrowski, F.; Evert, M. & Calvisi, D. F. Functional crosstalk between AKT/mTOR and Ras/MAPK pathways in hepatocarcinogenesis: implications for the treatment of human liver cancer. *Cell Cycle, 12(13)*:1999-2010, 2013.

Wang, F.; Fu, K.; Wang, Y.; Pan, C.; Wang, X.; Liu, Z.; Yang, C.; Zheng, Y.; Li, X.; Lu, Y.; *et al*. Small-molecule agents for cancer immunotherapy. *Acta Pharm. Sin. B, 14(3)*:905-52, 2024.

Wang, Y.; Shen, Y.; Wang, S.; Shen, Q. & Zhou, X. The role of STAT3 in leading the crosstalk between human cancers and the immune system. *Cancer Lett., 415*:117-28, 2018.

Xu, G.; Ye, X.; Chen, J. & Liu, D. Effect of heat treatment on the phenolic compounds and antioxidant capacity of citrus peel extract. *J. Agric. Food Chem., 55(2)*:330-5, 2007.

Xu, H.; Chen, K.; Shang, R.; Chen, X.; Zhang, Y.; Song, X. & Calvisi, D. F. Alpelisib combination treatment as novel targeted therapy against hepatocellular carcinoma. *Cell Death Dis., 12(10)*:920, 2021.

Yang, L.; Lei, S. & Xu, W. Rising above: exploring the therapeutic potential of natural product-based compounds in human cancer treatment. *Tradit. Med. Res., 10(3)*:18, 2025.

Younossi, Z. M. & Henry, L. Epidemiology of non-alcoholic fatty liver disease and hepatocellular carcinoma. *JHEP Rep., 3(4)*:100305, 2021.

Corresponding author:
Nael Abutaha
Department Zoology
College of Science
King Saud University
P.O. Box 2455
Riyadh 11451
SAUDI ARABIA

E-mail: nabutaha@ksu.edu.sa